Chinese Chemical Letters 35 (2024) 108795

Contents lists available at ScienceDirect

Chinese Chemical Letters

journal homepage: www.elsevier.com/locate/cclet

Anchoring heterometallic cluster on P-doped carbon nitride for efficient photocatalytic nitrogen fixation in water and air ambient

Chao-Long Chen, Rong Chen, La-Sheng Long, Lan-Sun Zheng, Xiang-Jian Kong*

Collaborative Innovation Center of Chemistry for Energy Materials, State Key Laboratory of Physical Chemistry of Solid Surfaces and Department of Chemistry, College of Chemistry and Chemical Engineering, Xiamen University, Xiamen 361005, China

ARTICLE INFO

Article history:
Received 8 March 2023
Revised 18 June 2023
Accepted 9 July 2023
Available online 11 July 2023

Keywords:
Photocatalytic
Nitrogen fixation
4f-3d
Cluster
Air atmosphere

ABSTRACT

Light-driven nitrogen fixation to produce ammonia is a green and economical technology of nitrogen reduction but is still quite challenging, especially in an air atmosphere without any sacrificial reagents. Herein, we demonstrate efficient photocatalytic nitrogen fixation using water and air directly by loading lanthanide–transition metal (4f–3d) cluster $NdCo_3$ on two-dimensional P-doped graphitic carbon nitrides (PCN) material surface. Benefiting from the increase in the number of nitrogen vacancies (NVs) and highly matched band gap structure and excellent hole trapping ability of clusters, the $NdCo_3$/PCN photocatalyst exhibits efficient nitrogen reduction activity with 371 (in air) and 825 μmol h^{-1} g^{-1} (in pure nitrogen) without any sacrificial reagents. The introduction of potassium sulfate inhibits hydrogen production and promotes nitrogen reduction activation. This work suggests that anchoring precisely structured clusters on 2D materials may enhance photocatalytic nitrogen reduction under normal temperature and pressure.

Nitrogen reduction reaction (NRR) has become a significant research topic because nitrogen is indispensable for various life forms [1,2]. The emergence of Haber-Bosch process allows humans to artificially use nitrogen to synthesize ammonia. However, owing to the robust N≡N triple-bonds, the process requires plenty of energy in the face of severe conditions and releases huge amounts of greenhouse gases into the atmosphere [3,4]. Photocatalytic nitrogen fixation is a hopeful and sustainable method of nitrogen reduction using solar power as raw energy [5]. Since the first study of TiO_2-controlled photo-reduction of dinitrogen was exhibited [6], numerous catalysts sprung up and have attracted the attention of the researchers, involving Vo-TiO_2, BiOBr, Bi_5O_7Br, LDHs, V-g-C_3N_4, Mo-$W_{18}O_{49}$, Au/MIL-100(Cr) and so on [4,7–12]. Although many efforts have resulted in tremendous achievements in this field, the photocatalytic efficiency of NRR is still inefficient on account of the low charge separation, the weak adsorption of nitrogen on catalytic sites, the side hydrogen production in the system, and so on. At present, it is hard to design efficient nitrogen fixation photocatalysts to realize the formation of ammonia under mild conditions, especially in air atmosphere without any sacrificial reagents.

Graphitic carbon nitride (C_3N_4) is an ideal photocatalyst because of its unique two-dimensional structure, appropriate band gap, and excellent stability [13]. A series of efficient C_3N_4-based photocatalysts have been designed by adjusting the defect sites and band gap or loading various metal nanoparticles [10,13–16]. Nitrogen vacancies (NVs) were confirmed to be effective catalytic sites for activated nitrogen [10,17]. However, such polydispersed nanoparticles make it tough to accurately modulate the electronic structure and active sites at the atomic level. Some examples of redox potential modulation by lanthanide/transition metals [18] and the effective involvement of transition metal-polyoxometalate catalysts in catalytic reactions had been reported [19–21]. Lanthanide–transition metal (4f–3d) clusters not only integrate multiple metal centers but also have atomically accurate structures, which offer an ingenious catalytic model for achieving synergistic reaction effects [22–25]. Recently, by assembling a bio-inspired heterometallic $LnCo_3$ clusters on P-doped carbon nitride (PCN), a composite system $LnCo_3$/PCN was obtained and realized a solar-driven overall water splitting in our previous work [26]. The $LnCo_3$ clusters not only act as the oxygen evolution center (OEC) but also its combination with PCN leads to a suitable band gap structure and high charge separation efficiency.

In this work, we introduced $NdCo_3$ clusters to enrich NVs in PCN and optimize charge separation efficiency. By adding K ions to suppress the hydrogen production and enhance nitrogen adsorption and activation in NVs, we realized efficient photocatalytic nitrogen fixation of $NdCo_3$/PCN photocatalyst under the direct utilization of water and air without sacrificial reagents. The $NdCo_3$/PCN shows efficient nitrogen fixation efficiency with 825

* Corresponding author.
E-mail address: xjkong@xmu.edu.cn (X.-J. Kong).

https://doi.org/10.1016/j.cclet.2023.108795
1001-8417/

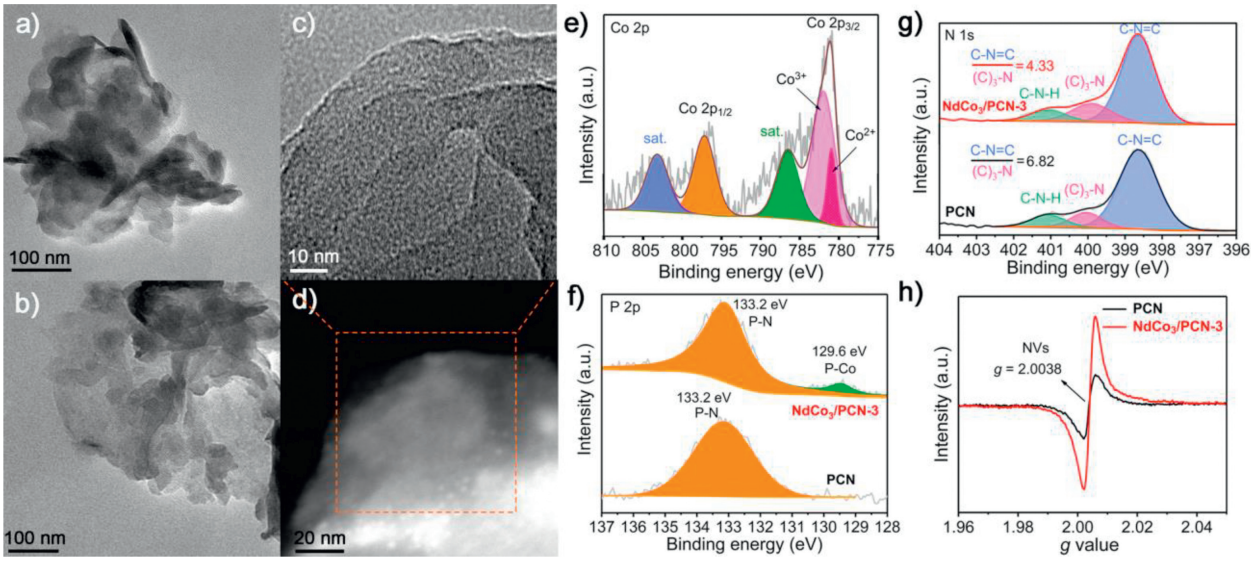

Fig. 1. TEM images of PCN (a) and $NdCo_3$/PCN-3 (b). HRTEM (c) and HAADF-STEM images (d) of $NdCo_3$/PCN-3, the orange selected area in (d) is the acquisition location of (c). (e) Co 2p XPS spectrum of $NdCo_3$/PCN-3. (f) P 2p XPS spectrum of PCN and $NdCo_3$/PCN-3. (g) N 1s XPS spectrums of PCN and $NdCo_3$/PCN-3. (h) EPR spectra of PCN and $NdCo_3$/PCN-3 at 100 K.

μmol h^{-1} g^{-1} (in pure nitrogen and potassium sulfate) under illumination, which was nearly 27 times as many as pure PCN in water. More interestingly, using a steady stream of air instead of high-purity nitrogen as the raw material for NRR, $NdCo_3$/PCN shows the high tolerance of oxygen with nitrogen fixation activity of 371 μmol h^{-1} g^{-1}. This study presents a brand-new strategy for nitrogen fixation in the air atmosphere by assembling lanthanide–transition clusters with photoactive supports.

Because of the stability of clusters in methyl alcohol, methyl alcohol was selected as the solvent to load the clusters on the semiconductor PCN by our reported method [26]. 3, 5, 7, 10, and 12 mg of clusters methanol solutions were added to 45 mg of PCN in methanol, respectively. The resulting compounds were named $NdCo_3$/PCN-1 (1.08 wt%), $NdCo_3$/PCN-2 (1.62 wt%), $NdCo_3$/PCN-3 (2.14 wt%), $NdCo_3$/PCN-4 (3.06 wt%), and $NdCo_3$/PCN-5 (3.63 wt%), which the actual clusters (based on Nd) loading quantity was defined by Inductively coupled plasma emission spectroscopy (ICP-OES), (Table S1 in Supporting information).

Fig. S1a (Supporting information) displays the powder X-ray diffraction (PXRD) patterns of PCN and $NdCo_3$/PCN-1, 2, 3, 4, and 5. The obvious peaks appear at 13.2° and 27.6°, which were identified as the (100) and (002) crystal planes of carbon nitride (C_3N_4) [27–29]. With the addition of clusters, the peak intensity at 13.2° and 27.6° is slightly weakened, but the crystal phase of the substrate is not changed, and the composite still maintains a stable structure. Scanning electron microscopy (SEM) images demonstrate that PCN and $NdCo_3$/PCN-3 appear in nanosheet morphology (Figs. S2a and c in Supporting information). Besides, the mapping graphics indicate that $NdCo_3$ is evenly distributed on the entire catalyst (Figs. S2d–g in Supporting information). Transmission electron microscopy (TEM) figures also showed that the photocatalyst exhibits two-dimensional nanosheet morphology (Figs. 1a and b). In order to confirm the dispersion of $NdCo_3$ cluster, the high-resolution TEM (HRTEM) and high-angle-annular-dark-field scanning transmission electron microscopy (HADDF-STEM) characterization experiment was performed. As shown in Figs. 1c and d, and Fig. S3 (Supporting information), single white dots that emerged on PCN were observed clearly, indicating that the $NdCo_3$ clusters were evenly dispersed throughout the substrate.

The characteristic peaks of Nd 3d and Co 3d are clearly observed in the X-ray photoelectron spectroscopy (XPS) full spectrum further confirming the loading of $NdCo_3$ clusters (Fig. S4a in Supporting information), and Co maintains two different valence states (Co^{3+} and Co^{2+}) (Fig. 1e). By comparing the P 2p XPS spectrum of PCN and $NdCo_3$/PCN-3, it is convinced that the $NdCo_3$ and PCN are firmly bonded through the Co-P bond (Fig. 1f) [30–32]. The PCN substrate still maintains a complete C–N frame structure (Fig. 1g and Fig. S4b in Supporting information) [33]. The XPS of N 1s was fitted and three peaks located at 398.6, 399.9, and 401.1 eV, corresponding to C–N=C, N-$(C)_3$, and C–N-H, respectively (Fig. 1g) [28,34]. The reduced ratio (from 6.82 to 4.33) of C–N=C/N-$(C)_3$ indicates that NVs occur preferentially at the positions of two-coordinated N (N_{2c}) and the increase in the number of NVs after doping [28]. The electron paramagnetic resonance (EPR) spectroscopy of PCN and $NdCo_3$/PCN-3 at g = 2.0038 (Fig. 1h) further confirms that the loading of clusters enriches the NVs [10,28,35].

Photocatalytic nitrogen reduction reactions (pNRR) in water under nitrogen or air atmosphere were carried out in a quartz container under light irradiation (300–800 nm, Fig. S5 in Supporting information). The NH_4^+ content was measured by the Nessler reagent method (Fig. S6 in Supporting information) and verified by ion chromatography (IC, Fig. S7 in Supporting information). As Fig. 2a shows, $NdCo_3$/PCN-3 exhibited NH_4^+ reaction rate of 256 μmol h^{-1} g^{-1} in pure water, which is nearly 8 times the amount of pure PCN in water (30 μmol h^{-1} g^{-1}). The abundant NVs play a key role. The other products after the reaction were also detected. As Table S2 and Fig. S8 (Supporting information) show, the hydrogen evolution reaction rate is about 307 μmol h^{-1} g^{-1}, suggesting that hydrogen evolution competition in the nitrogen reduction reaction is the main factor affecting the ammonia yield.

In order to suppress the production of hydrogen effectively, potassium ions were added in the photocatalytic system because the alkali ions can not only provide a powerful electric field to polarize N_2 and steady intermediate products, but also make the adsorption of N_2 and the desorption of NH_3 easier [36,37]. As shown in Fig. 2a, replacing pure water with potassium sulfate solution, the photocatalytic activity of $NdCo_3$/PCN-3 reached 825 μmol h^{-1} g^{-1}, nearly 27 times as many as pure PCN in water. Meanwhile, the production rate of hydrogen was greatly reduced to 70 μmol h^{-1} g^{-1}, and the effective utilization of electrons increased from 55.5% to 94.6%. These results indicate that adding K^+ is an efficient means of improving ammonia selectivity. With the increase

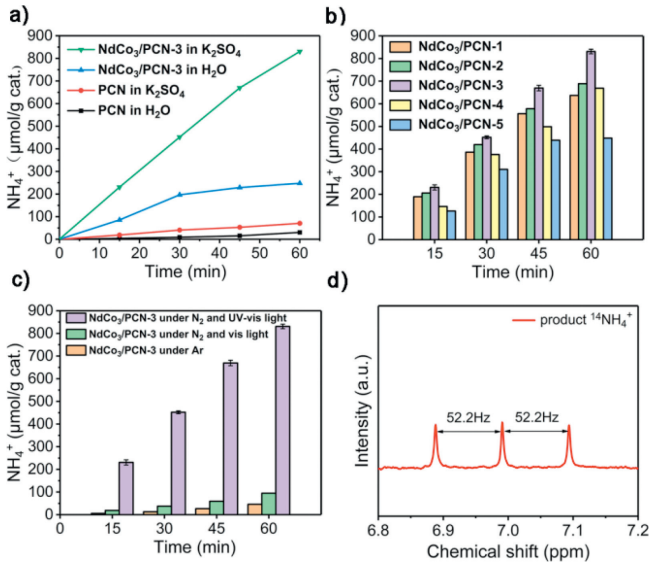

Fig. 2. (a) Ammonia production rate of PCN and $NdCo_3$/PCN-3 in pure water and 0.5 mol/L K_2SO_4 solution. (b) Ammonia production rate of $NdCo_3$/PCN with different loading in 0.5 mol/L K_2SO_4 solution. (c) Control experiments of $NdCo_3$/PCN-3 in 0.5 mol/L K_2SO_4 solution. (d) The reaction liquid's ^1H NMR spectra after the catalyst $NdCo_3$/PCN-3 reacting for 3 h in water.

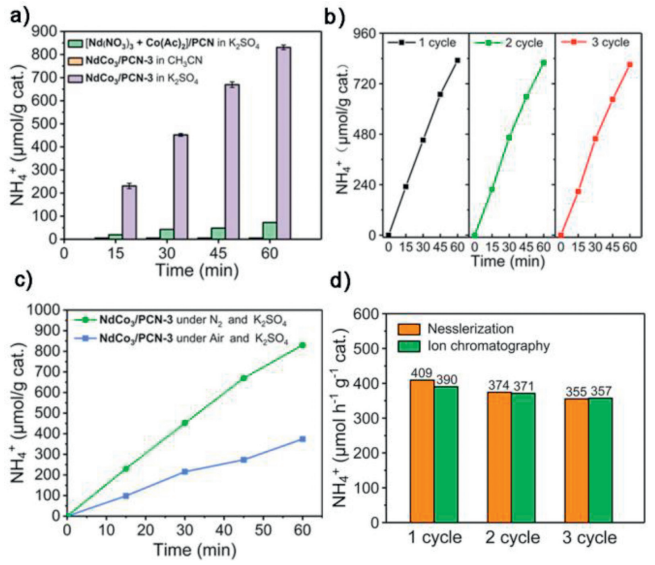

Fig. 3. (a) Control experiments of $NdCo_3$/PCN-3 for ammonia reduction. (b) Catalytic activity cycle experiment of $NdCo_3$/PCN-3 in 0.5 mol/L K_2SO_4 solution. (c) Ammonia production rate of $NdCo_3$/PCN-3 in air and N_2. (d) The cyclic experiments in air atmosphere were compared by ion chromatography and Nesslerization.

of $NdCo_3$ cluster loading on PCN, the separated efficiency of photo-induced carriers is greatly enhanced, given that $NdCo_3$/PCN-3 obtained the best performance (Fig. 2b). Further increasing the loading amount, the NH_4^+ production rate was decreased. The reason is that the competition between different clusters reduces the chance for holes to migrate to the same oxidation site.

To verify the source of ammonia, the control experiment with argon gas was studied. Without nitrogen, almost no ammonia signal is generated, confirming the origin of ammonia from nitrogen (Fig. 2c). The extremely small amount of ammonia is due to the background of the CN material [38,39]. By replacing the light source with visible light, only a relatively small amount of ammonia is produced (Fig. 2c). As shown in Fig. 2d and Fig. S9 (Supporting information), the ^1H NMR spectra of liquid product after the reaction of catalyst $NdCo_3$/PCN-3 in water for 3 h shows three typical split peaks of $^{14}NH_4^+$ (6.9–7.1 ppm), which further confirms that ammonium originates from N_2 [40,41]. To eliminate the possible contributions from interfering species, a control experiment of $[Nd(NO_3)_3 + Co(Ac)_2]$/PCN was studied using the same condition as $NdCO_3$/PCN. As Fig. 3a shows, $[Nd(NO_3)_3 + Co(Ac)_2]$/PCN showed a very low photocatalytic activity, which indicates that the effect of $NdCo_3$ enhanced the photocatalytic nitrogen fixation performance. Moreover, no NH_4^+ signal is observed with aprotic solvent CH_3CN instead of water in the control experiment, indicating the source of protons is indeed provided by water molecules. In addition, the stability of the catalyst also is explored. After three cycles of testing, catalytic activity did not decrease significantly (Fig. 3b), and the recycled catalyst $NdCo_3$/PCN-3 still maintains the original morphology and crystal phase (Fig. S10 in Supporting information), indicating that the synthesized catalyst has good stability. Energy dispersive spectroscopy (EDS) analysis of the catalyst after cycling was performed. As shown in Fig. S11 and Table S3 (Supporting information), elements Nd and Co are still present on the catalyst and the ratio is close to 1:3, confirming that $NdCo_3$ is still loaded on the PCN. Moreover, the reaction solution was tested by inductively coupled plasma mass spectrometry (ICP-MS). The results show that less than 0.4% of the metal ions enter the solution (Table S4 in Supporting information), further confirming that the $NdCo_3$ clusters are stable on the PCN. This stability comes from the fact that the composite catalyst $NdCo_3$/PCN is chemically bonded with P-Co.

Considering that the nitrogen content in air is very rich, the pNRR experiment was carried out in air atmosphere. Notably, the NH_4^+ formation rate of $NdCo_3$/PCN-3 in air without any additives was 371 μmol h^{-1} g^{-1}, and $NdCo_3$/PCN-3 revealed outstanding oxygen resistance (Fig. 3c). This tolerance stems from the fact that NVs are not disturbed by reactive oxygen species. Similarly, $NdCo_3$/PCN-3 still maintains a high catalytic stability in the air, and the accuracy of the catalytic yield data was tested by IC (Fig. 3d and Fig. S12 in Supporting information). Using inexhaustible air as the raw material to replace nitrogen to synthesize ammonia is rare in previous reports (Table S5 in Supporting information). This is the first attempt at photoreduction of nitrogen using a cluster-based composite catalyst in air and genuinely obtains chemical energy from nature under mild conditions. To separate the photogenerated carriers effectively, methanol was used to capture the photogenerated holes. The ammonia yield has almost doubled and can maintain a stable output for a long time, which confirmed that the transfer of holes is a key step and clusters play a vital role in trapping holes (Fig. S13 in Supporting information). The oxidation products of methanol have also been studied (Fig. S14 in Supporting information), most are formaldehyde, with a small part of formic acid. The accuracy of all the above catalytic yields was verified by IC (Fig. S7 in Supporting information). According to Watt and Chrisp's method, no N_2H_4 was detected in the reaction solution, suggesting that the catalyst also has high selectivity of reduction of ammonia (Fig. S15 in Supporting information).

One of the key factors affecting photo-catalytic efficiency is the charge separation and transfer of photo-induced carriers. To measure the charge separation efficiency, the electrochemical impedance spectra (EIS) and transient photocurrent response (TPC) were performed. As shown in Fig. 4a, the Nyquist diagrams of $NdCo_3$/PCN-3 show a lesser radius and lower interfacial charge transfer resistance compared to PCN. Compared to PCN, $NdCo_3$/PCN-3 also displays an excellent photocurrent response (Fig. 4b), suggesting that $NdCo_3$/PCN-3 has high electron-hole separation and transfer efficiency. Photoluminescence and time-resolved fluorescence spectrum (Figs. 4c and d) show the

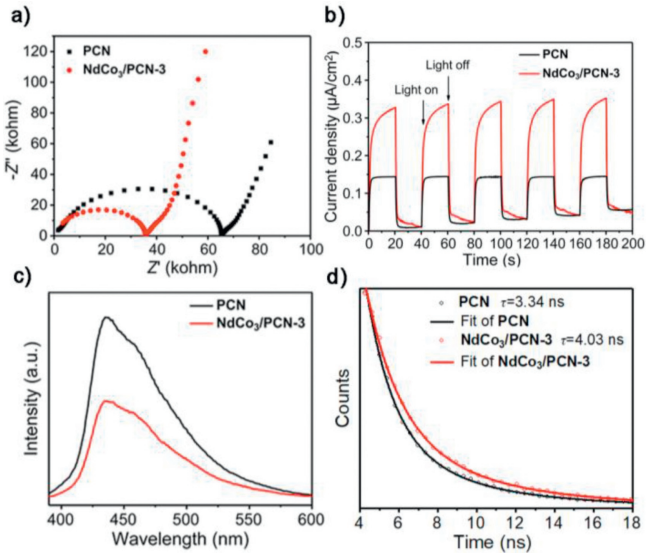

Fig. 4. (a) EIS of PCN and $NdCo_3$/PCN-3. (b) Transient photocurrent responses of PCN and $NdCo_3$/PCN-3 under simulated irradiation. (c) Photoluminescence spectra of PCN and $NdCo_3$/PCN-3 with excitation at 368 nm. (d) Time-resolved fluorescence spectrums of PCN and $NdCo_3$/PCN-3 at room temperature with excitation and emission at 368 and 430 nm, respectively.

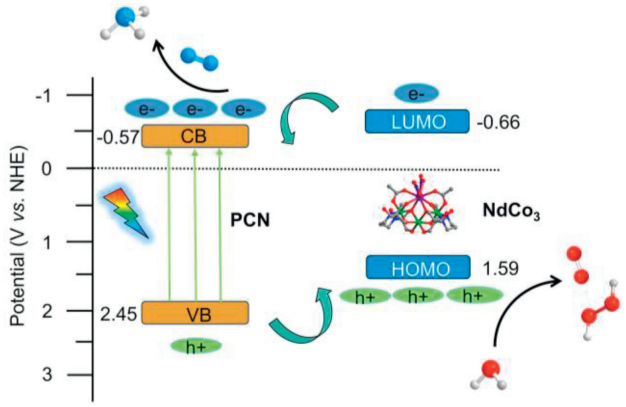

Fig. 5. Separation of photo-induced carriers under full-band exposure with $NdCo_3$/PCN composite.

weaker energy emission transition and longer average lifetime of $NdCo_3$/PCN-3, indicating that the loading of $NdCo_3$ on PCN can enhance photo-induced electron-hole separation velocity and restrain carrier recombination.

The interfacial charge transfer mechanism between atomically accurate nanoclusters and semiconductor substrates was studied [42,43]. In our previous work, it has been confirmed that $NdCo_3$ is the active center of oxidation process [26]. According to calculation (Figs. S16 and S17 in Supporting information), the band gap width and the energy band position of $NdCo_3$ and PCN were shown in Fig. 5. When the light-sensitive PCN substrate is exposed under illumination, the photo-induced electrons were rapidly motivated to conduction band (CB), while the remaining holes were quickly shifted to the HOMO energy level of $NdCo_3$ due to the highly matched valence band (VB). The loading of $NdCo_3$ restrains photo-induced electron-hole recombination of PCN efficiently and completes the oxidation process of water, producing oxygen and hydrogen peroxide (Figs. S8 and S18 in Supporting information). Correspondingly, the electrons on the LUMO energy level of $NdCo_3$ were transferred to CB of PCN and efficiently injected into nitrogen's antibonding orbital which adsorbed and activated by NVs, completed the reduction of nitrogen. Profiting from photo-induced electron-hole separation and utilization effectually and abundant NVs, the integral catalytic efficiency has been improved and got a satisfactory result.

In summary, an efficient oxidation center $NdCo_3$ cluster was anchored on PCN nanosheets, which significantly increased the active site NVs and enhanced photo-induced carriers transport of PCN. Without any scavengers and co-catalysts, the $NdCo_3$/PCN-3 exhibited high NRR activity with 355 μmol h^{-1} g^{-1} in air atmosphere and 825 μmol h^{-1} g^{-1} in pure nitrogen. The $NdCo_3$/PCN composites show suitable energy band structure and prominent reducing the power of controlling electrons. This work suggests that anchoring precisely structured clusters on 2D materials may enhance photocatalytic nitrogen reduction under normal temperature and pressure.

Declaration of competing interest

The authors declare that there is no interest for this manuscript.

Acknowledgment

This work was supported by the National Natural Science Foundation of China (Nos. 21871224, 92161104, 92161203, and 21721001).

Supplementary materials

Supplementary material associated with this article can be found, in the online version, at doi:10.1016/j.cclet.2023.108795.

References

[1] P.C. Dos Santos, R.Y. Igarashi, H.I. Lee, et al., Acc. Chem. Res. 38 (2005) 208–214.
[2] M.A. Legare, G. Belanger-Chabot, R.D. Dewhurst, et al., Science 359 (2018) 896–900.
[3] A. Banerjee, B.D. Yuhas, E.A. Margulies, et al., J. Am. Chem. Soc. 137 (2015) 2030–2034.
[4] Y.X. Zhao, Y.F. Zhao, R. Shi, et al., Adv. Mater. 31 (2019) 1606482.
[5] Y. Nishibayashi, M. Saito, S. Uemura, et al., Nature 428 (2004) 279–280.
[6] G.N. Schrauzer, T.D. Guth, J. Am. Chem. Soc. 99 (1977) 7189–7193.
[7] H. Li, J. Shang, Z.H. Ai, L.Z. Zhang, J. Am. Chem. Soc. 137 (2015) 6393–6399.
[8] S.Y. Wang, X. Hai, X. Ding, et al., Adv. Mater. 29 (2017) 1701774.
[9] Y.F. Zhao, Y.X. Zhao, G.I.N. Waterhouse, et al., Adv. Mater. 29 (2017) 1703828.
[10] G.H. Dong, W.K. Ho, C.Y. Wang, J. Mater. Chem. A 3 (2015) 23435–23441.
[11] N. Zhang, A. Jalil, D.X. Wu, et al., J. Am. Chem. Soc. 140 (2018) 9434–9443.
[12] Y.N. Liu, X.Y. Ye, R.P. Li, et al., Chin. Chem. Lett. 33 (2022) 5162–5168.
[13] C. Liang, H.Y. Niu, H. Guo, et al., Chem. Eng. J. 406 (2021) 126868.
[14] P.X. Qiu, C.M. Xu, N. Zhou, H. Chen, F. Jiang, Appl. Catal. B 221 (2018) 27–35.
[15] X.H. Li, W.L. Chen, P. He, et al., Inorg. Chem. Front. 6 (2019) 3315–3326.
[16] F. Chu, Y.Z. Hu, K.Y. Zhang, et al., J. Colloid Interface Sci. 634 (2023) 159–168.
[17] W.W. Lin, H. Chen, G.B. Lin, et al., Angew. Chem. Int. Ed. 61 (2022) e202207807.
[18] K.Y. Zhang, F. Chu, Y.Z. Hu, et al., Chin. Chem. Lett. 34 (2023) 107766.
[19] Y.J. Wang, G.L. Zhuang, J.W. Zhang, et al., Angew. Chem. Int. Ed. 62 (2023) e202216592.
[20] Y.T. Song, Y.W. Peng, S. Yao, et al., Chin. Chem. Lett. 33 (2022) 1047–1050.
[21] H.Q. Yin, L.L. Yang, H. Sun, et al., Chin. Chem. Lett. 34 (2023) 107337.
[22] X.Y. Zheng, X.J. Kong, Z.P. Zheng, L.S. Long, L.S. Zheng, Acc. Chem. Res. 51 (2018) 517–525.
[23] R. Chen, Z.H. Yan, X.J. Kong, L.S. Long, L.S. Zheng, Angew. Chem. Int. Ed. 57 (2018) 16796–16800.
[24] R. Chen, Z.H. Yan, X.J. Kong, ChemPhotoChem 4 (2020) 157–167.
[25] Z.H. Pan, Z.Z. Weng, X.J. Kong, L.S. Long, L.S. Zheng, Coord. Chem. Rev. 457 (2022) 214419.
[26] R. Chen, G.L. Zhuang, Z.Y. Wang, et al., Natl. Sci. Rev. 8 (2021) nwaa234.
[27] X.W. Feng, H. Chen, F. Jiang, X. Wang, J. Colloid Interface Sci. 509 (2018) 298–306.
[28] C.D. Lv, Y.M. Qian, C.S. Yan, et al., Angew. Chem. Int. Ed. 57 (2018) 10246–10250.
[29] Z.Q. Liang, Y.C. Guo, Y.J. Xue, H.Z. Cui, J. Tian, Mater. Chem. Front. 3 (2019) 2032–2040.
[30] W. Liu, L.L. Cao, W.R. Cheng, et al., Angew. Chem. Int. Ed. 56 (2017) 9312–9317.
[31] Y.J. Zhang, T. Mori, J.H. Ye, M. Antonietti, J. Am. Chem. Soc. 132 (2010) 6294–6295.
[32] W. Liu, E.Y. Hu, H. Jiang, et al., Nat. Commun. 7 (2016) 10771.
[33] Y. Ran, X.L. Yu, J.Q. Liu, et al., J. Mater. Chem. A 8 (2020) 13292–13298.
[34] H.J. Yu, R. Shi, Y.X. Zhao, et al., Adv. Mater. 29 (2017) 1605148.

[35] Z.H. Hong, B. Shen, Y.L. Chen, B.Z. Lin, B.F. Gao, J. Mater. Chem. A 1 (2013) 11754–11761.
[36] Y.C. Hao, Y. Guo, L.W. Chen, et al., Nat. Catal. 2 (2019) 448–456.
[37] T.A. Bu, Y.C. Hao, W.Y. Gao, et al., Nanoscale 11 (2019) 10072–10079.
[38] W.K. Wang, H.M. Zhang, S.B. Zhang, et al., Angew. Chem. Int. Ed. 58 (2019) 16644–16650.
[39] W.K. Wang, H.J. Zhou, et al., Small 16 (2020) 1906880.
[40] Y. Fang, Y.R. Xue, L. Hui, H.D. Yu, Y.L. Li, Angew. Chem. Int. Ed. 60 (2021) 3170–3174.
[41] R.Y. Hodgetts, A.S. Kiryutin, P. Nichols, et al., ACS Energy Lett. 5 (2020) 736–741.
[42] Y. Wang, X.H. Liu, Q.K. Wang, et al., Angew. Chem. Int. Ed. 59 (2020) 7748–7754.
[43] C.L. Chen, H.Y. Wang, J.P. Li, et al., Inorg. Chem. Front. 9 (2022) 2862–2868.